lubricants

MDPI

Article

Influence of Additives Concentration on the Electrical Properties and the Tribological Behaviour of Three Automatic Transmission Fluids

Alejandro García Tuero [1], Noelia Rivera [2], Eduardo Rodríguez [1], Alfonso Fernández-González [3], José Luis Viesca [1] and Antolín Hernández Battez [1,*]

[1] Department of Construction and Manufacturing Engineering, University of Oviedo, Pedro Puig Adam s/n, 33203 Gijón, Spain
[2] Department of Marine Science and Technology, University of Oviedo, Blasco de Garay, s/n, 33203 Gijón, Spain
[3] Department of Physical and Analytical Chemistry, University of Oviedo, Julián Clavería 8, 33006 Oviedo, Spain
* Correspondence: aehernandez@uniovi.es

Abstract: Placing an electric motor (EM) inside the transmission housing of a hybrid electric vehicle (HEV) implies that the automatic transmission fluid (ATF) needs to accomplish additional requirements. Among these requirements, electrical compatibility is of critical significance. This study investigated the influences of the additive concentrations of three commercial ATFs on their electrical compatibilities and tribological performances. Two variations of each ATF with different concentrations of the original additive packages were prepared. The viscosity, electrical conductivity, permittivity, resistivity, dielectric dissipation factor, breakdown voltage, and tribological performance of the nine resulting ATFs were measured. All the ATFs were found to be electrically compatible and showed dissipative performance and sufficiently high breakdown voltage, even at increasing additive concentrations. The tribological performances of the ATFs formulated with the API (American Petroleum Institute) Group III base oils had improved wear reduction at the highest additive concentrations; the better wear performance was related to the formation of iron phosphates and polyphosphates on the worn surface.

Keywords: electric vehicles; automatic transmission fluid; electrical properties; additives; friction; wear

Citation: García Tuero, A.; Rivera, N.; Rodríguez, E.; Fernández-González, A.; Viesca, J.L.; Hernández Battez, A. Influence of Additives Concentration on the Electrical Properties and the Tribological Behaviour of Three Automatic Transmission Fluids. *Lubricants* **2022**, *10*, 276. https://doi.org/10.3390/lubricants10110276

Received: 5 October 2022
Accepted: 19 October 2022
Published: 22 October 2022

1. Introduction

The transportation sector is one of the main sources of greenhouse gas (GHG) emissions, according to the European Environmental Agency (EEA) [1] and the US Environmental Protection Agency (EPA) [2]. The agencies report that 27% and 22% of the total GHG emissions are from this sector (in their respective geographical areas). For this reason, taking action in this sector, especially on road transportation, is a key step toward achieving the targets of the 2030 Agenda for sustainable development [3]. Vehicle electrification is the main option to accomplish this goal. The main reason for the high impact of electric vehicles (EV) on GHG emissions reduction is their higher efficiency [4] when compared to ICE (internal combustion engine) vehicles. However, in addition to full EVs, HEVs (hybrid electric vehicles) play an important role in the transition to the zero-emissions by 2035 scenario determined at the Conference of the Parties (COP26) [5].

The layout of the configuration of an HEV includes the electric motor (EM) inside the mechanical transmission housing. In this case, the automatic transmission fluid (ATF) must meet numerous requirements. Apart from reducing friction and wear, the ATF used in a HEV must protect against corrosion, avoid foaming and aeration at high speeds, have good cooling properties, and be compatible with electric and magnetic fields and the polymers used as seals and structural materials [6,7]. The selection of base oils and the type and concentration of additives are essential to fulfil the above-mentioned requirements.

Gao et al. [8] patented a lubricant for HEVs and EVs with no more than 20 wt% of additives, which is able to maintain the electrical conductivity (κ) and kinematic viscosity within desirable values. Previously, Flores-Torres et al. [9] patented a method for preventing electrostatic problems within EV powertrains. According to this method, the lubricant must have at least one base oil (API Groups I to V), one additive package, and at least one conductivity agent, which could be included in the additive pack. The base oil should be at least 70 wt% of the total amount of the lubricant, and the additive pack between 0.01 and 30 wt%. The additive package, which is formulated under the manufacturer's criteria, must have at least one of the following additives: antioxidant, detergent, dispersant, antiwear, corrosion inhibitor, viscosity modifier, or a metal passivator. In these circumstances, the κ of the lubricant should be between 10 and 20,000 pS/m and the kinematic viscosity between 2 and 20 cSt at 100 °C.

The concentration of the additive exerts influence on the tribological performance of the lubricant and the fulfilment of the special requirements for an ATF to be used in an electrified driveline. The κ of the fully formulated oils (FFO) is considerably affected by the additive composition, concentration, and chemistry at similar viscosities, while viscosity must be considered for κ control as it becomes lower [10]. On the other hand, the ZDDP (zinc dialkyldithiophosphate) included in the lubricants as an antiwear additive can be activated by increasing the κ, although the support of other additives, such as tetradecylammonium tetrakis-(4-fluorophenyl)-borate (TDATPhFB) is necessary to improve this property [11]. This effect could also be achieved with a polar aprotic solvent, such as sodium dodecyl sulphate (SDS) and ionic liquid additives [12,13].

On the other hand, the improvement of tribological behaviour by means of a given additive concentration can worsen other properties, such as κ and dielectric strength, which are very important in HEV cases with EMs inside the transmission housing. When considering the hypothesis that conventional ATFs used in ICE vehicles are not suitable to fulfil the requirements of the abovementioned HEV cases, it is useful to determine how different concentrations of the additive package can affect both tribological and electrical properties. The aim of this study was to investigate the combined effects of the additive concentrations in three conventional ATFs on their electrical and tribological properties. The compatibility of these ATFs with structural polymers and elastomers and the oxidation influences of these ATFs on their electrical conductivities were previously studied [14–16]. The novelty (and practical application) of this research consists of studying the feasibility of using conventional ATFs in HEVs and observing how changing the additive concentrations of one property can be improved without worsening another one (to an unacceptable value), which is important for both academic and industry stakeholders.

2. Experimental Details

2.1. Materials

Three commercial–automatic transmission fluids (ATFs) were used as reference oils (ATFs A, B, and C); their properties are listed in Table 1. ATF A was composed of a mixture of two mineral oils (SP90H and LN-100HS) from API Group I as a base fluid and the additive package EDR-219. Meanwhile, ATFs B and C were composed of a mixture of two mineral oils (YUBASE 3 and YUBASE 6) from API Group III as base fluids and the additive packages HiTEC 3460 and HiTEC 3488, respectively. The chemical elements included in the additive packages were determined for the three abovementioned ATFs and the results are reported in Table 2.

Table 1. Properties of the automatic transmission fluids.

ATFs	Base Oils (wt. %)	Additive (wt. %)	Kinematic Viscosity (mm^2/s)		Viscosity Index
			40 °C	100 °C	
A	88.80	11.20	44.3	8.0	154
A0	80.00	20.00	68.5	11.8	169
A1	95.00	5.00	34.4	6.2	130
B	89.00	11.00	28.5	5.8	152
B0	80.00	20.00	37.1	7.2	161
B1	95.00	5.00	24.4	5.0	135
C	83.00	17.00	33.8	7.1	180
C0	80.00	20.00	37.6	7.8	184
C1	90.00	10.00	26.2	5.7	168

Table 2. Content of the additive elements in the non-modified commercial ATFs.

Additive Elements	Standards	ATF A	ATF B	ATF C
Ca, ppm	ASTM D 4951	150–240	–	170–220
B, ppm	ASTM D 4951	78	59–88	140–210
P, ppm	ASTM D 4951	160–250	136–194	410–540
Zn, ppm	ASTM D 4951	–	20	–
S, %	ISO 8754		0.192	0.066
N, %	ASTM D 5291	0.105–0.162	–	–

Two additional lubricant samples were studied for each ATF, changing the base fluid concentration by approximately ± 9%, except in the case of ATF C0, whose base fluid concentration decreased by 3.7%. Thus, three lubricant samples with a base fluid/additive ratio of 80/20 (expressed in wt.%) were studied, and other lubricant samples with higher and lower base fluids/additive ratios were also analysed. The mixtures of the base oils and the additive packages were prepared in a planetary centrifugal mixer (Kakuhunter SK-300 SII) for 30 min at 1600 rpm.

2.2. Viscosity and Electrical Property Measurements

The viscosities of the different ATFs were measured from 20 to 100 °C, every 10 °C, in a Stabinger SVM 3001 viscometer (Anton Paar, Graz, Austria). The temperature range was selected by considering the temperatures that were potentially reached inside the transmission (by gears) and in the main parts of the EM (if the latter was included in the transmission housing). The potential temperatures that could be reached in the EM were reported in a recent paper [14].

The electrical conductivities of the abovementioned lubricant samples were measured at 40, 60, 80, and 100 °C with a digital conductivity meter (Emcee Model 1153 (Emcee Electronics, Inc., Venice, FL, USA)). At least three electrical conductivity measurements were made for each lubricant sample. The dielectric breakdown voltage was measured at room temperature. VDE (Verband Deutscher Elektrotechniker) electrodes were used, with a separation of 2.5 mm. The tension at the electrodes increased by 2 $kV \cdot s^{-1} \pm 0.2$ $kV \cdot s^{-1}$ and the uncertainty of the measuring equipment was 4.3 kV. The volume of the lubricant sample was approximately 400 mL; the electrodes were completely covered in oil, and the lubricant sample was subjected to continuous mechanical agitation. All of these parameters correspond to the EN 60156 standard. The resistivity (ρ), relative permittivity (ε), and dielectric dissipation factor (tan δ) were measured at room temperature (25 °C) with an LCM calculator v3.0 by Alff Engineering. The frequency was 50 Hz, and the measurements were made according to the UNE-EN (IEC) 60247 standard.

2.3. Tribological Tests

All the lubricant samples were tested in a Mini Traction Machine (MTM2 (PCS Instruments, London, UK)) performing two different tests: the so-called Stribeck curve

determination and the traction test. The Stribeck curves were obtained at 40, 60, 80, and 100 °C for an entrainment speed range of 10–2500 mm·s^{-1}. The load was set at 25 N, which implied a maximum contact pressure of 0.9 GPa. The slide-to-roll ratio (SRR) was 100%. The traction tests were performed under the same loads and temperatures as the Stribeck curve tests, but they were performed at a continuous entrainment speed of 2000 mm·s^{-1}. The SRR values increased periodically from 0 to 100%.

Equations (1) and (2) define the entrainment speed and SRR, respectively. The difference between the tangential speed of the disc (u_{disc}) and the ball (u_{ball}) at the point of contact determines the entrainment speed (V_S). The volume of the lubricant used in each test was 10 mL. The balls (9.525 mm-radius) and discs (23 mm-radius) were made of AISI 52100 steel, with a maximum surface roughness of 0.020 µm.

$$Vs = u_{disc} - u_{ball} \tag{1}$$

$$SRR = 2 \cdot \frac{|(u_{disc} - u_{ball})|}{(u_{disc} + u_{ball})} \times 100\% \tag{2}$$

Ball-on disc reciprocating friction and wear tests were also performed in a CETR UMT-3 (San José, CA, USA) tribometer. The properties of the specimens used in these tribological tests were: balls of 6 mm-diameter, 58–66 HRC hardness, and 0.05 µm Ra surface roughness; and discs of 10 mm-diameter, 190–210 HV30 hardness, and 0.018 µm Ra surface roughness. Both specimens were manufactured from AISI 52100 steel. The tribometer was configured with a 4 mm stroke length and a frequency of 15 Hz. The duration of the tests was 60 min, the fluid temperature was set at 100 °C, and the load was 10 N (corresponding to 1.43 GPa of maximum contact pressure). The coefficient of friction (COF) was instantaneously recorded, and the wear volume was measured on the disc's surface with a confocal microscope (Leica DCM 3D (Leica Biosystems, Wetzlar, Germany)). Each test was performed at least twice with a fresh lubricant sample and new specimens. Before and after all tribological tests, the specimens were ultrasonically cleaned in heptane for 10 min, rinsed in ethanol, and then air-dried with hot air.

2.4. Worn Surface Characterization

The worn surface was analysed by scanning electron microscopy and energy dispersive spectroscopy (SEM/EDS) with a JEOL JSM-5600 (Jeol, Tokyo, Japan) unit, which operated at 15 kV. The wear mechanism and the elemental chemical composition of the worn surface were determined by using these techniques, respectively. Later, the surface lubricant chemical interaction was studied by X-ray photospectroscopy (XPS) with a monochromatic X-ray source equipped with an Al cathode (1486.7 eV). Survey spectra were taken at a pass-energy of 90 eV and 1 eV step energy, whereas high-resolution spectra were measured at 30 eV of pass-energy and a resolution (step energy) of 0.1 eV. The size spot of the X-ray source was about 2 mm^2 and focused on the wear scar, to avoid information of the unlubricated area.

3. Results and Discussions

3.1. Viscosity and Electrical Properties

Figure 1a shows the electrical conductivity (κ) behaviour of ATFs A, A0, and A1 with the temperature. The κ values are representative of the dissipative behaviours and the differentiations between the lubricant samples can be observed at increasing temperatures and changing additive concentrations. ATF A0 shows the highest κ values, corresponding with its higher additive concentration and, on the contrary, ATF A1 shows the lowest κ values. These changes in κ are below one order of magnitude, so they can be considered small. Figure 1b shows the dynamic viscosity behaviours of these ATFs with the temperature. Differences between the ATFs in the viscosity values were found over the whole temperature range, being higher at lower temperatures. At higher temperatures, the differences in viscosity between the lubricant samples were lower, while the higher

the additive concentration, the higher the viscosity values. Therefore, the differences in κ values at high temperatures were mainly related to the additives concentration and not to the different viscosities (Figure 1a,b). This conclusion about the influence of additives on the κ values was reported by Kwak et al. [10] and Chen et al. [15]. The so-called Walden plot (Figure 1c) shows that independently of the additive content used and, thus, independently of the κ of the sample, all the lubricant samples remained in the sub-ionic regime.

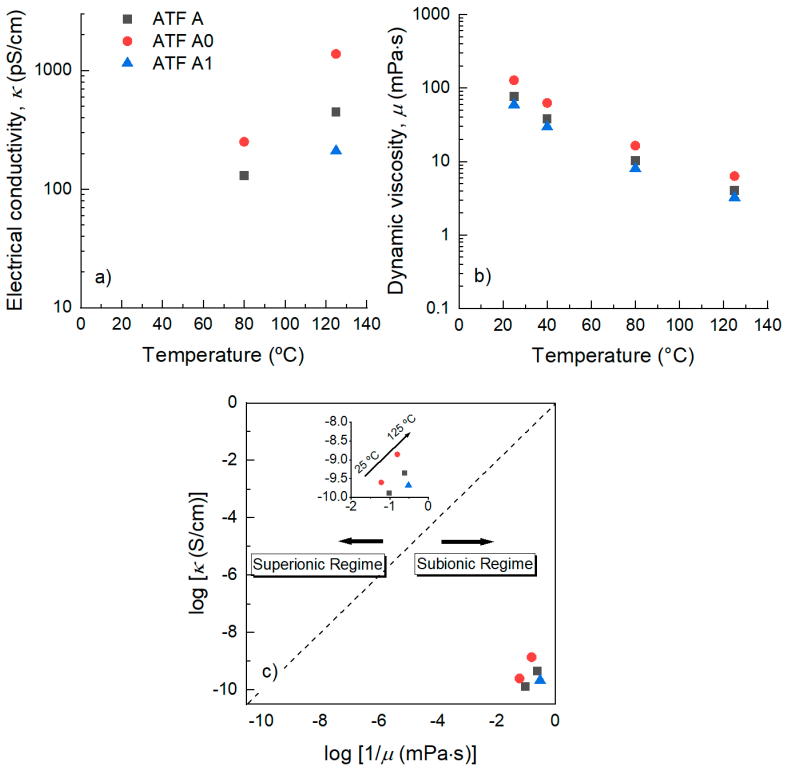

Figure 1. Electrical conductivity/viscosity/temperature relationships of ATFs A, A0, and A1.

The κ values of ATFs B, B0, and B1 (Figure 2) showed similar trends to those found in their counterparts A, A0, and A1. This similarity could be based on their identical additives concentration and no influence of the base oil could be identified. However, the κ values of ATFs B, B0, and B1 were higher than those of A, A0, and A1, likely due to the influence of the lower viscosity of the former. On the other hand, the κ values of ATFs C, C0, and C1 also bring out the influence of the additives (type and concentration) on the κ of fully formulated oils (Figure 3). ATF C0 showed lower κ values than ATF B0, having the same base oil/additive ratio and base oils from API Group III, but a different additive package. In addition, ATFs C and C1 showed higher κ values than ATF B and B1 due to a higher concentration and a different additive package. Thus, the composition of the additive package is also relevant for the κ value.

Independently of the base oils used, all the ATFs showed stronger dependencies of κ on the type and concentration of the additive package than on the oil viscosity. The relationship between the κ values of these fully formulated oils and their viscosities (at given temperatures) positions all of these ATFs in the sub-ionic regime; their κ values classify them as dissipative lubricants.

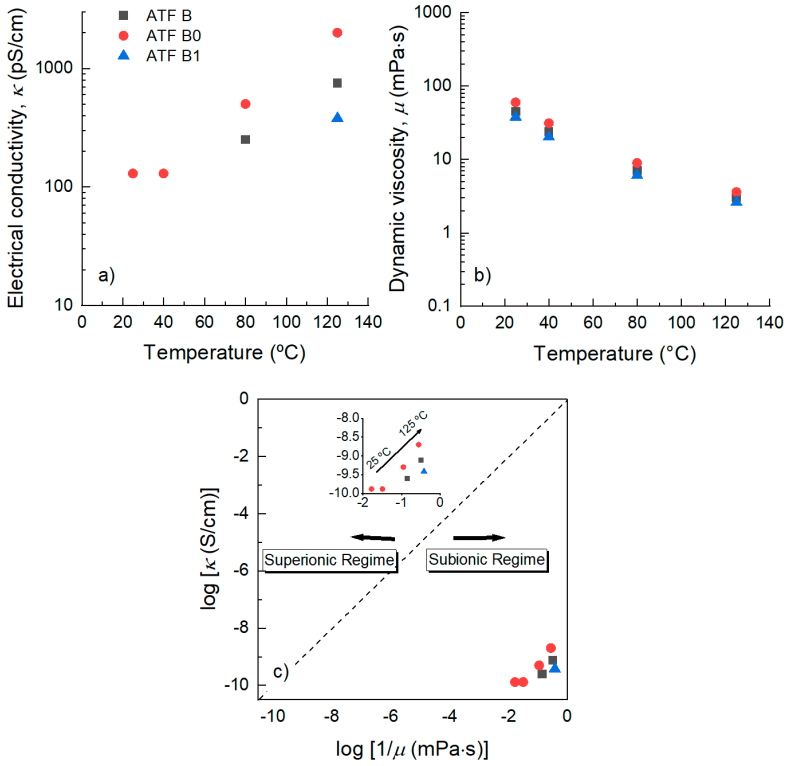

Figure 2. Electrical conductivity/viscosity/temperature relationships between ATFs B, B0, and B1.

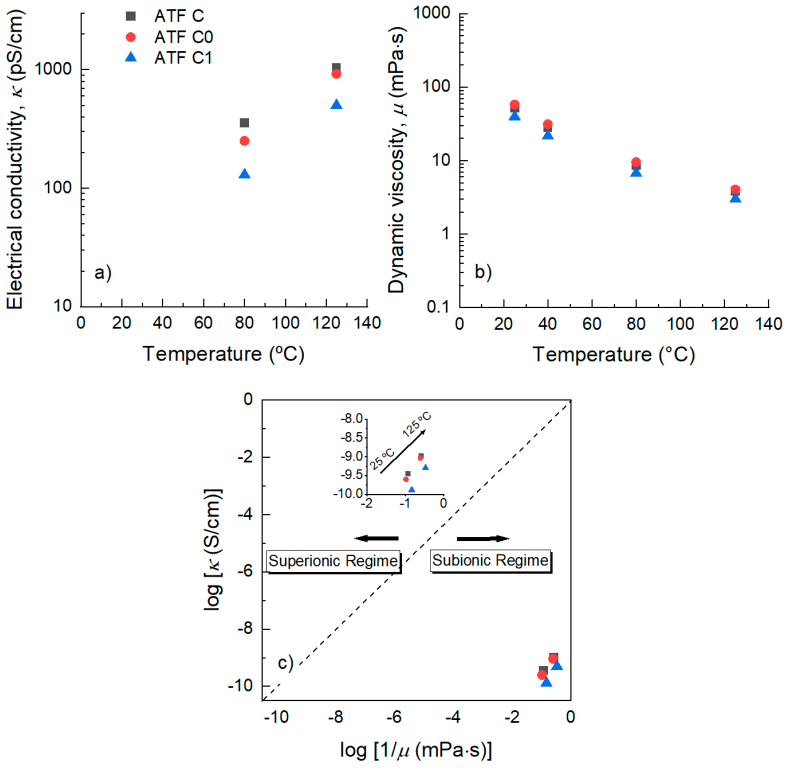

Figure 3. Electrical conductivity/viscosity/temperature relationships between ATFs C, C0, and C1.

The resistivity, permittivity, and dielectric dissipation factors (or tan δ) of the lubricant samples were measured at 20, 40, 60, 80, 90, and 100 °C. In addition, the dielectric breakdown voltage was also measured at room temperature (25 °C). The results of these measurements are presented in Figures 4–6.

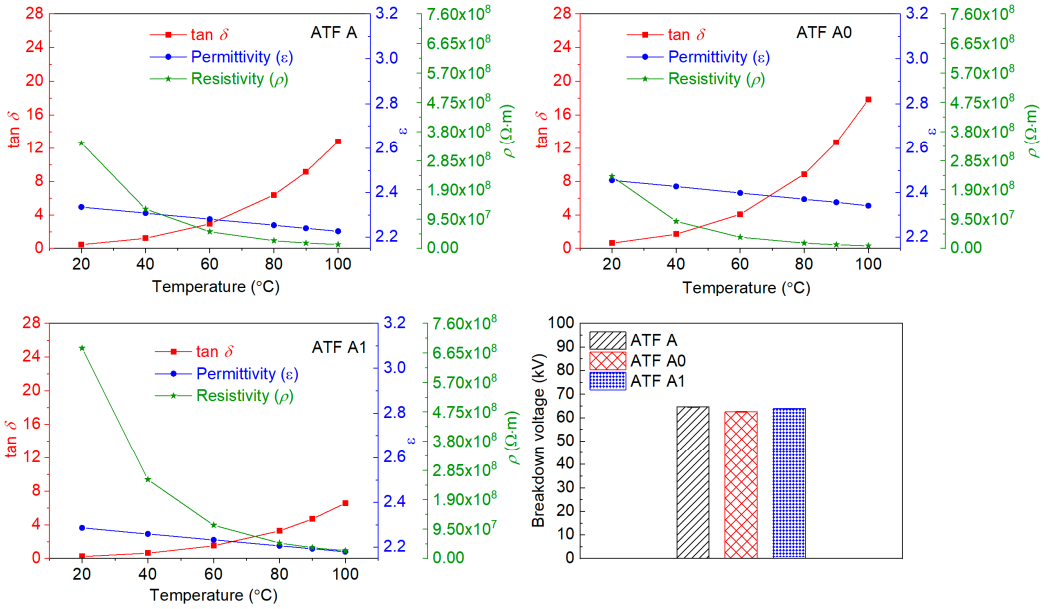

Figure 4. Dielectric properties of ATFs A, A0, and A1.

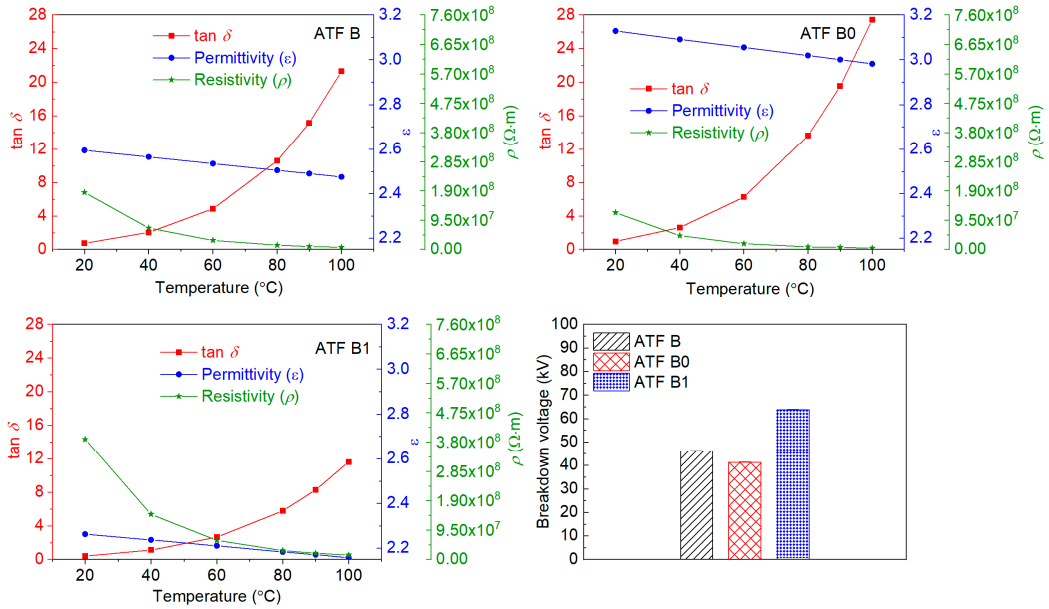

Figure 5. Dielectric properties of ATFs B, B0, and B1.

The resistivity of the base oils at room temperature is ~10^{13} Ω·m [16], while the values measured in all the lubricant samples are within the range 10^{7}–10^{8} Ω·m. These differences are due to some additives (antifriction, antiwear, detergent, corrosion inhibitor, and antioxidant) commonly used in the formulation of the ATFs, such as zinc dialkyldithiophosphates (ZDDP), molybdenum dialkyl dithiocarbamate (MoDTC), and magnesium alkyl sulfonate. These additives increase the polarity of the ATF, and the number and type of carriers, resulting in a huge reduction in the resistivity of the finished ATF [17]. The detections of zinc (Zn), phosphorus (P), sulphur (S), calcium (Ca), and boron (B) in the ATFs used in this work, Table 2, confirm the presence of the additive types abovementioned, (although it is not possible to specify which compound was used). This explains why the lubricant samples with the higher additive concentrations (ATFs A0, B0, and C0) showed the lowest resistivity values, and on the contrary, ATFs A1, B1, and C1 showed the highest resistivity values. In addition, the resistivity decreased by around one order of magnitude when the temperature increased from 20 to 100 °C. This is due to the fall in viscosity with the

increasing temperature; it can be observed that the higher the viscosity decreases with the temperature (samples with lower viscosity indices), the higher the decrease in resistivity and, thus, the higher the increase in electrical conductivity. The resistivity of an ATF, such as the electrical conductivity, should not be too high or too low, in order to avoid excessive current leakage (if resistivity is too low) and a possible discharge if a build-up of charge cannot be dissipated (if resistivity is too high).

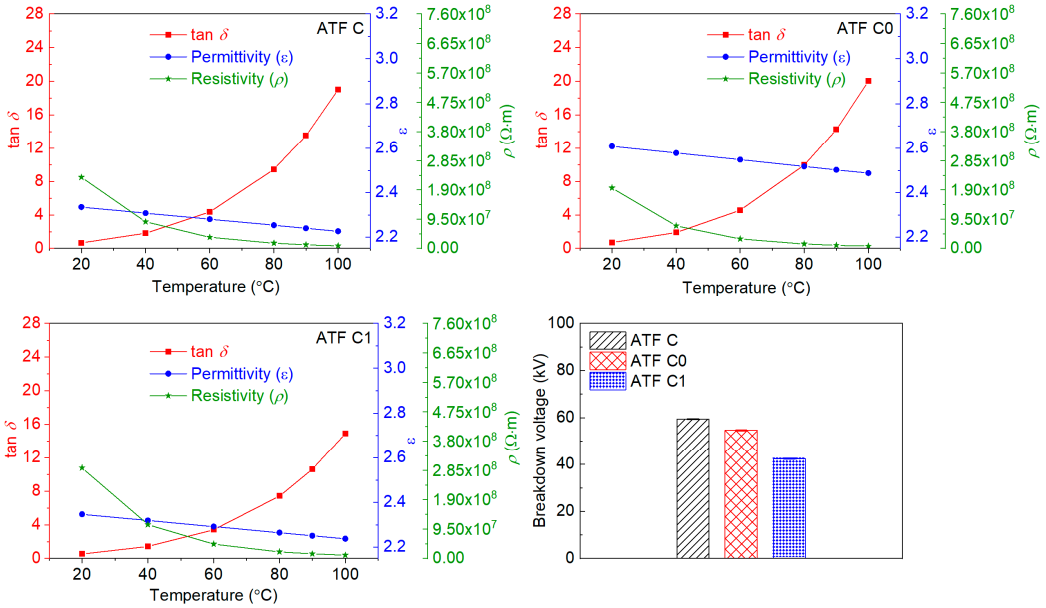

Figure 6. Dielectric properties of ATFs C, C0, and C1.

As expected, the temperature dependence of the permittivity of the ATFs was very weak, decreasing only around 4% when the temperature increased from 20 to 100 °C. However, the permittivity showed a strong proportional relationship with the additive concentration, especially in the B ATFs. By contrast, the tan δ of the ATFs was more sensitive to temperature, and also varied proportionally with the additive concentration.

Regarding the breakdown voltage, the obtained results indicate that the ATFs are safe for use in electric vehicles, where the rated voltage of the EM is typically below 1 kV. For this property, a correlation with the additive concentration was not found when considering the results shown by ATFs B and C.

3.2. Tribological Tests

The tribological behaviours of the three commercial ATFs and the corresponding lubricant samples with changes in the additive concentrations were studied by means of three different tests: Stribeck curve determination and traction tests performed under rolling/sliding conditions, and friction and wear tests under reciprocating motion conditions.

The Stribeck curve tests show how a lubricant performs under different contact conditions leading to distinct lubrication regimes (from hydrodynamic to boundary lubrication). As expected, the transition from elastohydrodynamic lubrication (EHL) to mixed lubrication (ML) occurs at a higher speed when the temperature rises, Figures 7–9. Under the EHL regime, the lubricant samples derived from each commercial ATF (ATFs A, B, and C) showed similar friction coefficients independently of the initial temperature of the test. This could be related to the similar viscosity of the lubricant samples, which controlled the lubricant film thickness. On the other hand, the differences in the friction coefficient under the mixed lubrication regime between the lubricant samples of each commercial ATF can be explained by the effect of increasing/decreasing additive concentrations on lubricant viscosity and/or tribofilm formation. The lubricant samples from ATFs A (Figure 7) and

C (Figure 9) showed slight friction differences, with the exception of ATF C0, in which its higher additive concentration seemed to reduce the possible shear-thinning rheological behaviour, resulting in higher lubricant viscosity and, thus, lower friction values. This could also explain the friction behaviour shown by ATFs B and B0 (Figure 8). In summary, the effects of the additive concentration on friction values under the ML regime depend on the rheological behaviour of the base oil, the viscosity increment with additive concentration, and the tribofilm formation due to the additive–surface chemical interaction.

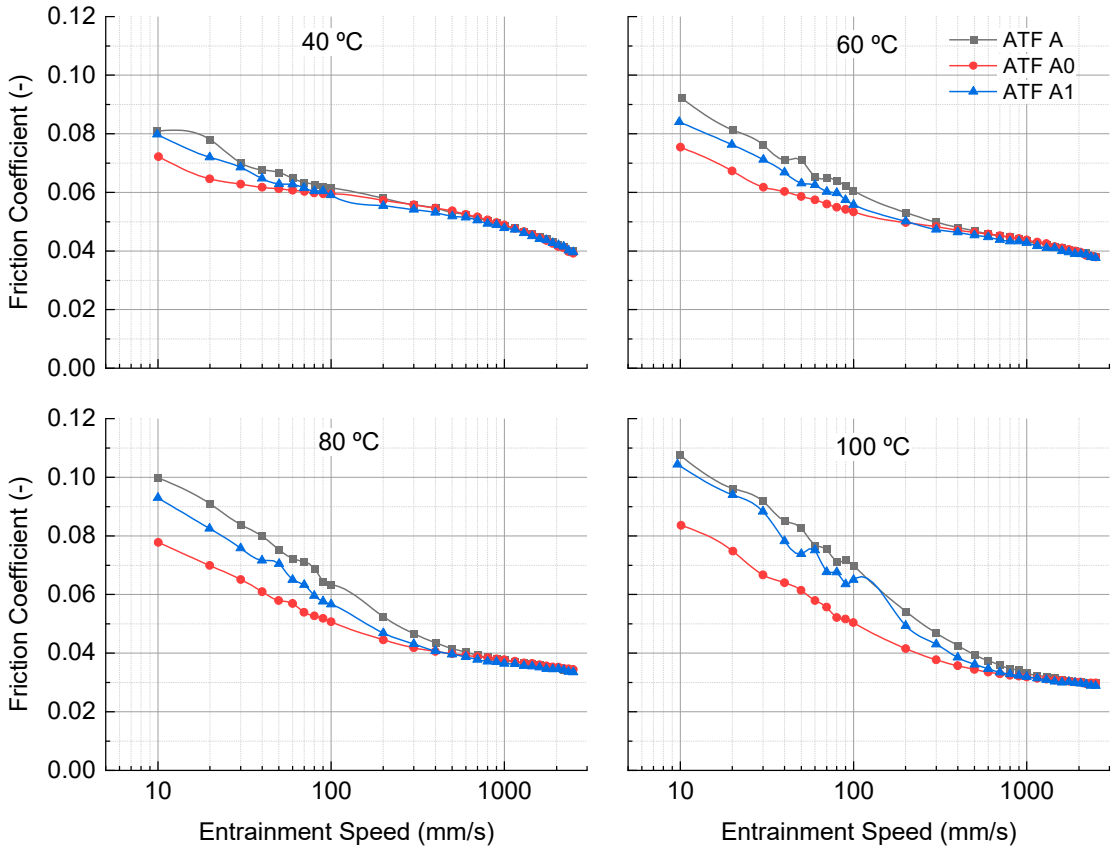

Figure 7. Stribeck curves of ATFs A, A0, and A1.

The traction properties of the ATFs are shown in Figure 10. Both the high entrainment speed and low-medium SRR conditions used led this test to be performed under a hydrodynamic lubrication regime, where friction was controlled by the lubricant viscosity. The small viscosity differences of ATFs A, A0, and A1, and possible shear-thinning rheological behaviour, resulted in no differentiation of the traction coefficient of these lubricant samples at the temperatures tested. In addition, ATFs B, B0, and B1 showed lower traction coefficient values than their counterparts A, A0, and A1 due to the lower viscosities of the former. ATFs C, C0, and C1 showed similar traction coefficient values at each temperature tested and these traction results were also similar to those of ATFs B, B0, and B1. In general, the changes in additive concentrations hardly affected the traction properties of the ATFs studied.

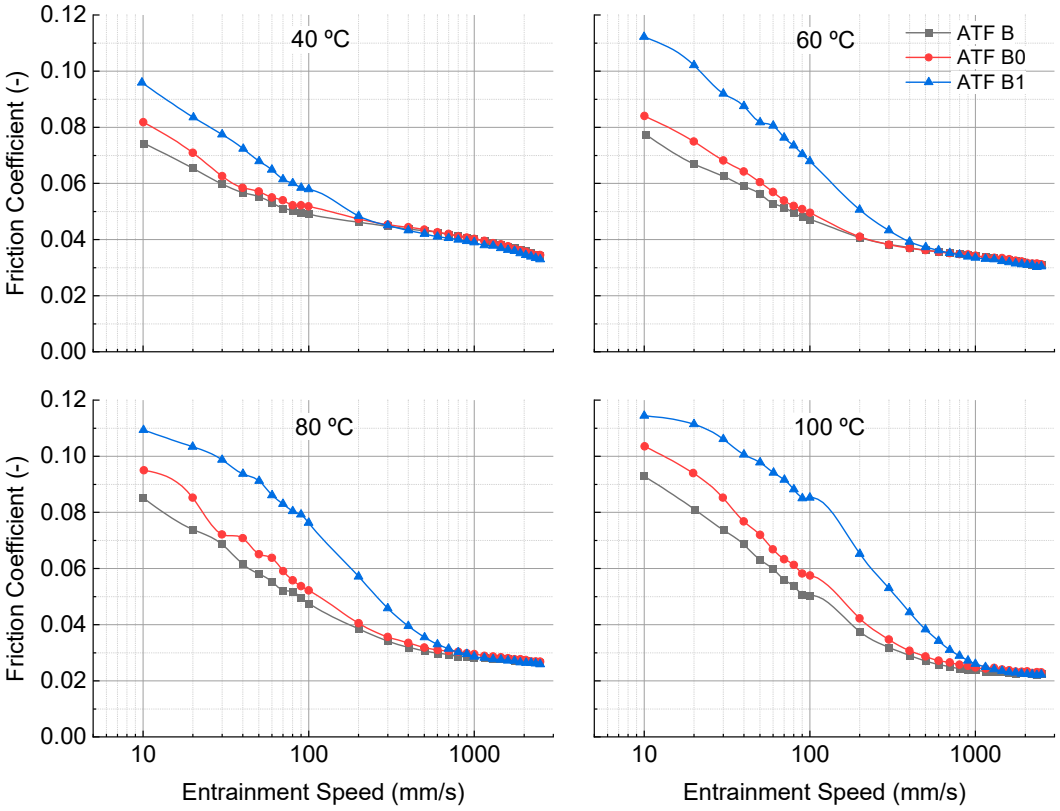

Figure 8. Stribeck curves of ATFs B, B0, and B1.

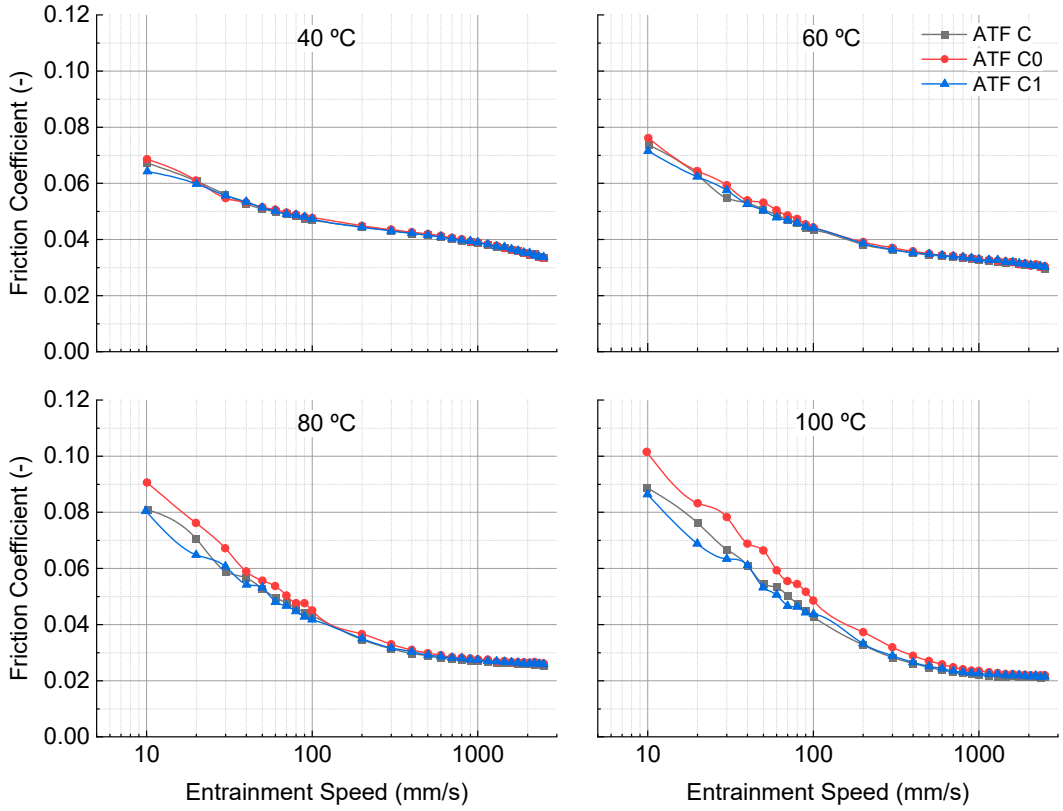

Figure 9. Stribeck curves of ATFs C, C0, and C1.

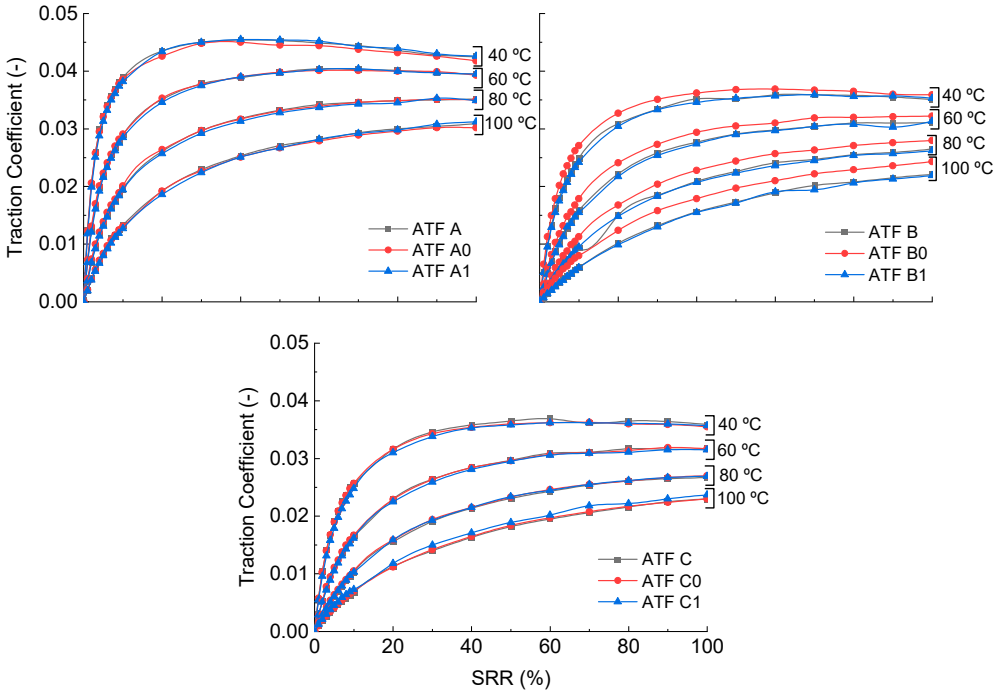

Figure 10. Traction curves of the ATFs.

Figure 11 shows the results of the friction and wear tests. The friction and wear behaviour of the ATFs could be explained in a similar way to that of ZDDP-containing fully formulated oils, where under a mixed lubrication regime most tribofilms formed are composed of phosphates, sulphates, and sulphides of Fe/Zn [18]. Higher antiwear additive concentrations, which correspond with a higher additive package concentration, can lead to two scenarios: (1) higher viscosity values, resulting in a thicker lubricant film and lower COF, or (2) a higher probability of tribofilm formation resulting in a possible inhibition of fluid film entrainment and, thus, thinner lubricant film and higher COF [19]. Both scenarios lead to less wear. On the contrary, lower antiwear additive concentrations can result in the opposite. ATF A0, with a higher additive concentration than A, showed a significantly higher COF and, thus, slightly higher wear, while the lower additive concentration of ATF A1 led to double the wear obtained with ATF A, even showing similar COF values. This could be explained by the fact that the two abovementioned scenarios are not mutually exclusive. For lubricant sample B, the one with the highest additive content (ATF B0) showed similar COF and slightly lower wear values than those of ATF B. Finally, ATF C0 showed the best antiwear behaviour and similar COF values of the C lubricant samples. In general, the antiwear behaviours of ATF B and C can be improved if the additive concentration is raised, while this solution worsens the friction reduction properties of ATF A.

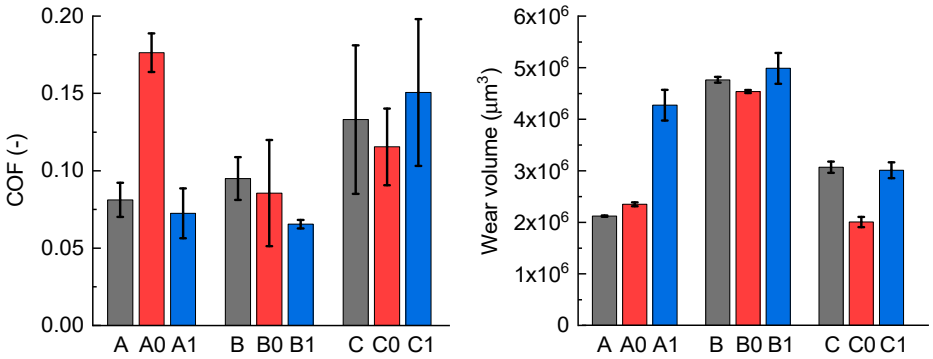

Figure 11. Average coefficient of friction and wear volume in friction test samples with all the ATFs.

3.3. Worn Surface Characterization

The SEM images of the worn surface after friction and wear tests with ATFs A, A0, and A1 show that the wear mechanisms were adhesive, and more plastic deformation was found at the edge of the worn surface after testing with ATF A1, Figure 12. The elemental analysis of the worn surface detected phosphorous when using ATFs A and A0, Table 3. On the contrary, this element was not found for ATF A1 at the detection limit of the EDS technique, which may explain the greater wear (Figure 11) found with this lubricant sample.

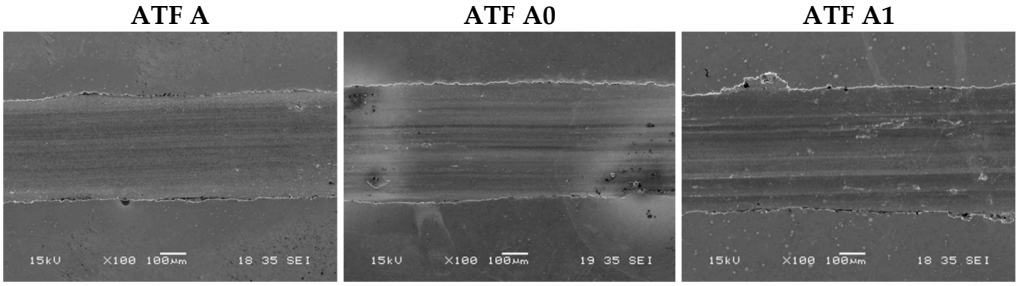

Figure 12. SEM of the worn surface after friction and wear tests with ATFs A, A0, and A1.

Table 3. EDS analysis from the wear scar on the disc after friction and wear tests with oils A.

ATF	Concentrations of Chemical Elements (wt%)							
	C	O	Si	P	Ca	Cr	Mn	Fe
ATF A	3.43	14.33	0.44	0.78	0.18	2.81	0.54	76.44
ATF A0	3.62	8.44	0.26	0.50	-	0.90	-	84.28
ATF A1	5.78	10.32	0.29	-	0.29	2.95	0.61	79.76

The wear mechanisms found after tests with ATFs B, B0, and B1 were similar to those for ATFs A, A0, and A1, Figure 13. No P was found by the EDS analysis technique (Table 4); nonetheless, taking into account the detection depth of this technique, P could still be found nearer to the surface at a lower concentration than in the tests with ATFs A, A0, and A1. The higher wear with ATFs B, B0, and B1, with respect to their counterparts A, A0, and A1, could be related to the lower amount of phosphorous found.

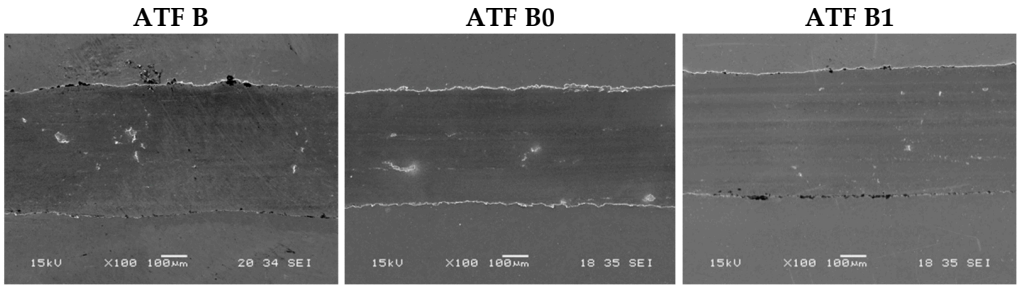

Figure 13. SEM of the worn surface after the tribological tests with ATFs B, B0, and B1.

Table 4. EDS analysis from the wear scar on the disc after friction and wear tests with oil B.

ATF	Concentration of Chemical Elements (wt%)								
	C	O	Si	P	S	Cr	Mn	Fe	Zn
ATF B	6.88	10.41	0.16	-	0.73	2.90	0.64	78.28	-
ATF B0	3.29	9.04	-	-	3.35	3.19	0.64	79.62	0.88
ATF B1	5.4	7.20	0.20	-	0.48	2.76	0.97	82.99	-

ATFs C, C0, and C1 showed the same wear mechanisms as the other ATFs (Figure 14), even with P being found in similar concentrations for all cases through the EDS analysis (Table 5). The lower wear obtained with the ATF C0 must be studied further.

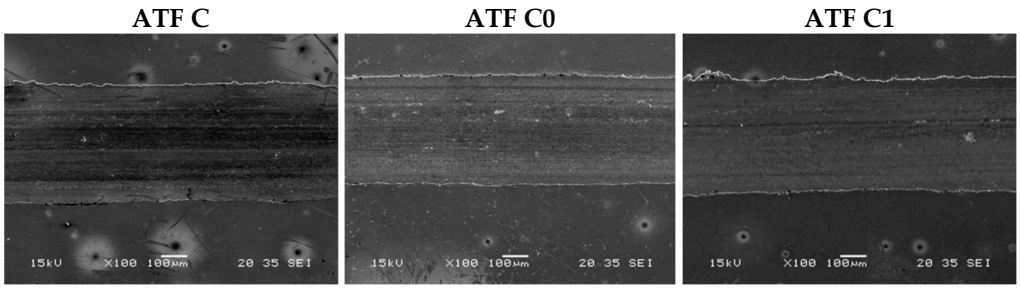

Figure 14. SEM of the worn surface after the tribological test with ATFs C, C0, and C1.

Table 5. EDS analysis from the wear scar on the disc after friction and wear tests with oil C.

ATF	Concentrations of Chemical Elements (wt%)								
	C	O	Si	P	S	Ca	Cr	Mn	Fe
ATF C	4.44	11.94	0.41	0.57	0.32	-	3.29	1.04	77.98
ATF C0	4.69	10.28	0.21	0.59	0.30	-	2.22	0.39	81.34
ATF C1	5.29	8.96	0.25	0.58	0.59	0.35	2.86	0.68	80.44

XPS was performed in order to verify the results obtained from the EDS analysis and confirm the chemical states of the elements on the wear scar. The results of the XPS measurements can be observed in Figures 15–17.

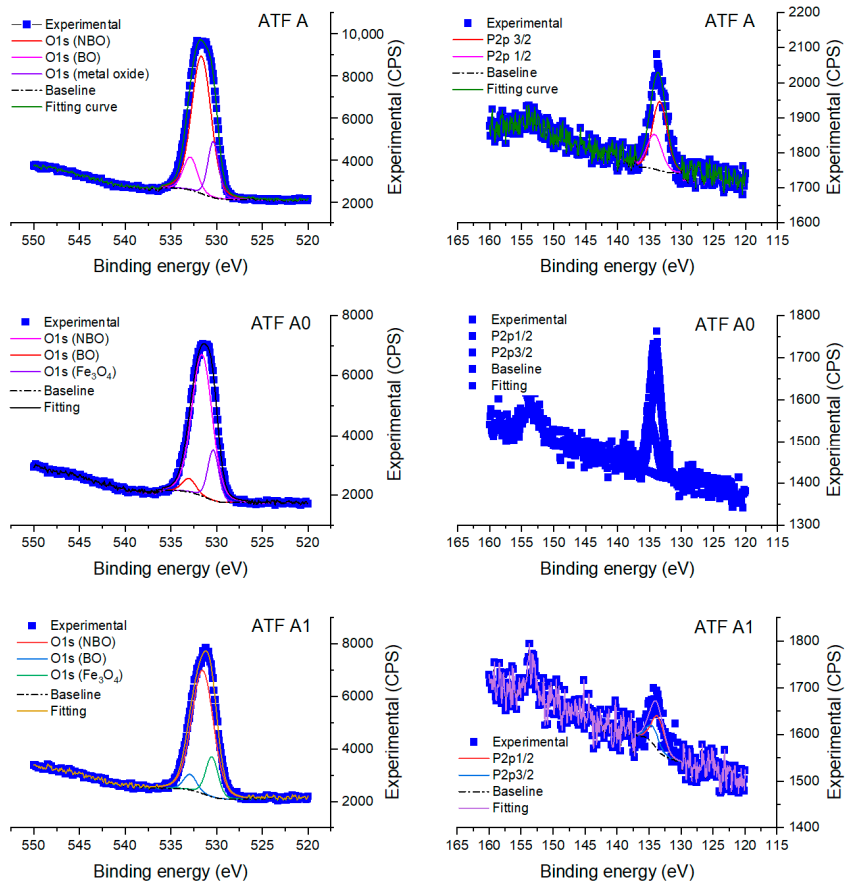

Figure 15. XPS spectra of P2p and O1s on the worn surface after tribological tests with ATFs A, A0, and A1.

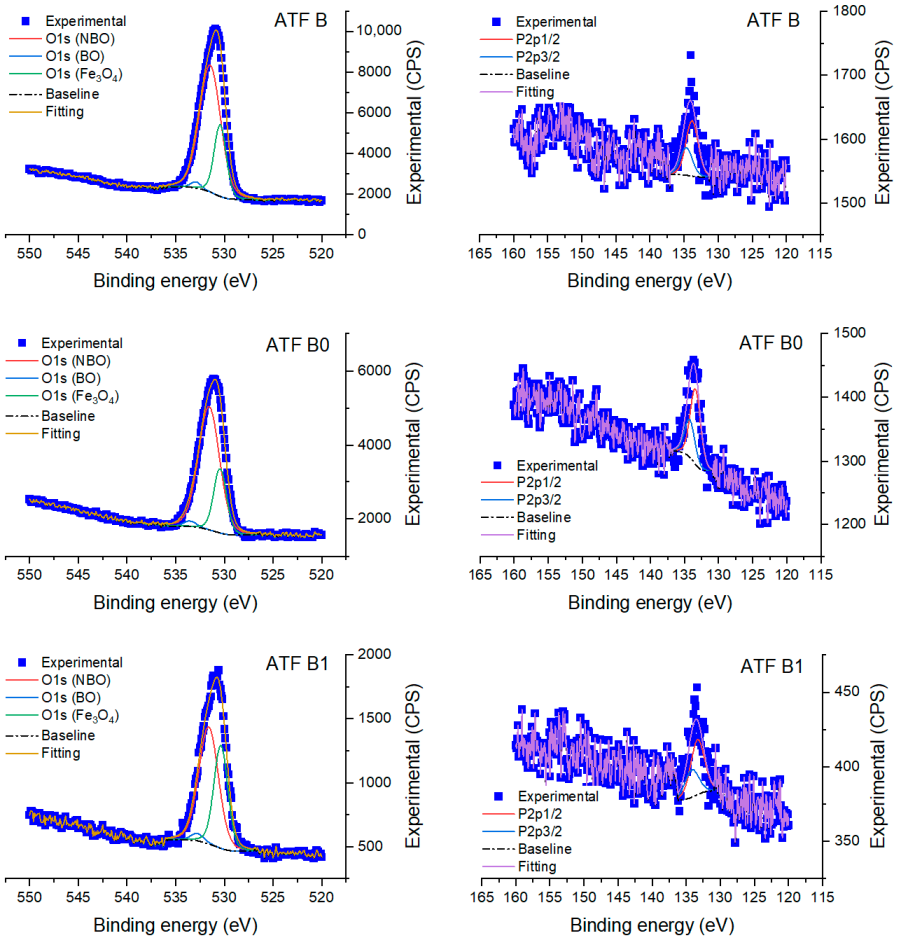

Figure 16. XPS spectra of P2p and O1s on the worn surface after tribological tests with ATFs B, B0, and B1.

The XPS analysis of the worn surface on the disc after tribological tests with oil A is shown in Table 6. The worn surfaces on the discs after tribological tests with ATF oil A, with different additive loads, were scanned at high resolutions for P2p and O1s peaks. The analysis revealed the presence of a P peak between 133.4 and 133.8 eV for ATFs A, A0, and A1, which is assignable to iron phosphate [20]. This compound is easily formed after reactions of phosphate compounds with steel [20] and is known to be an excellent wear-resistant species [21]. These results seem to agree with the phosphorus content of the additive lubricant (reported in Table 3), where the sample with the lowest concentration of this element (ATF A1) is also the sample with the higher worn wear volume.

O1s high-resolution spectra for ATF A fitted according to the positions described by Massoud et al. [22] for non-bridging oxygen with a P–O structure (NBO, at 531.6 ± 0.3 eV), bridging oxygen with a P–O–P structure (BO at 533.3 ± 0.3 eV), and metallic oxide (MO at 530.0 ± 0.3 eV), which show very similar compositions (Table 6). Deeper studies would be needed to accurately identify the kind of metal oxide formed, although according to Li et al. [23], it is most likely Fe_3O_4. This information is congruent with the presence of phosphates as detected in the P2p peaks, with the presence of bridging oxygen and polyphosphate characteristics at very low ratios.

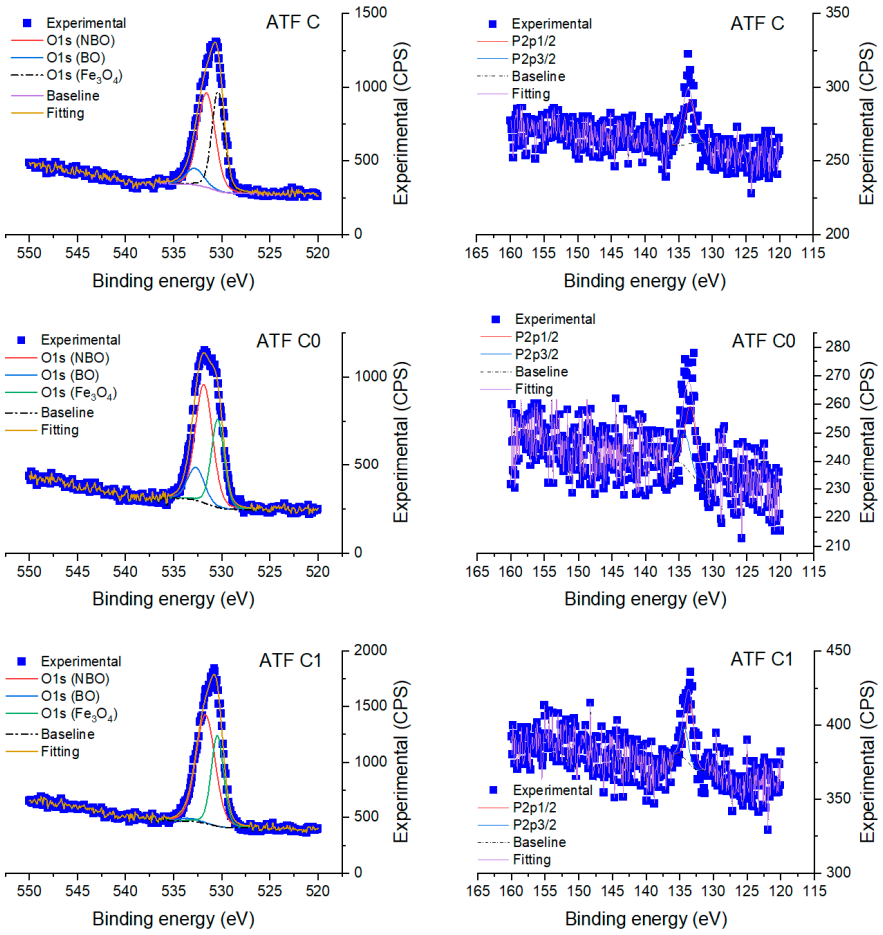

Figure 17. XPS spectra of P2p and O1s on the worn surface after tribological tests with ATFs C, C0, and C1.

Table 6. Peak positions, FWHM (Full Width at Half Maximum), and corresponding peak assignments for the O1s and P2p spectra under ATFs A, A0, and A1.

ATF	BE/eV	FWHM/eV	Area Percentage	Assigned to
		O1s		
A	531.7	2.5	71%	NBO
	532.9	1.8	12%	BO
	530.4	1.4	16%	Fe_3O_4
A0	531.6	2.6	80%	NBO
	533.0	1.8	5%	BO
	530.4	1.4	15%	Fe_3O_4
A1	531.5	2.8	79%	NBO
	532.9	1.6	6%	BO
	530.5	1.6	15%	Fe_3O_4
		P2p		
A	133.4	2.8	100%	$FePO_4$
A0	133.9	1.9	100%	$FePO_4$
A1	133.6	2.3	100%	$FePO_4$

Table 7 shows the XPS analyses of the worn surfaces after the tribological tests made with ATFs B, B0, and B1, which, with respect to oxygen and phosphorus, are very similar to those of ATFs A, A0, and A1 (Table 7). The presence of iron phosphates seems to be evident from the P2p and O1s spectra, as well as the presence of Fe_3O_4, although the presence of polyphosphates (assumed to appear as P–O–P) was even lower for oil B than for oil A. We should note that the worst wear behaviour of oil B is presented by ATF B1 (Figure 8), which is also the sample with the lowest content of iron phosphates (60% versus 75% for B and B0).

Table 7. Peak positions, FWHM, and corresponding peak assignments for O1s and P2p spectra under ATFs B, B0, and B1.

ATF	BE/eV	FWHM/eV	Area Percentage	Assigned to
		O1s		
B	531.4	2.6	76%	NBO
	532.9	1.3	2%	BO
	530.4	1.5	24%	Fe_3O_4
B0	531.6	2.5	74%	NBO
	533.5	1.5	2%	BO
	530.4	1.5	24%	Fe_3O_4
B1	531.6	2.4	60%	NBO
	532.8	1.6	2%	BO
	530.4	1.7	38%	Fe_3O_4
		P2p		
B	133.8	2.1	100%	$FePO_4$
B0	133.4	1.8	100%	$FePO_4$
B1	133.3	2.4	100%	$FePO_4$

Considering the composition of the additives (Table 2), the S2p XPS region was also scanned for ATFs B, B0, and B1 searching for the presence of sulphates. However, sulphur could not be detected on the surface of the samples, probably because of the low concentration of the element in the additive package. This seems to be a contradiction with the presence of sulphur detected with EDS (Table 4), but XPS is a surface analysis area whose depth is in the nanometre range, whereas EDS has a larger penetration. Taking into account the phenomenological model of the tribofilms generated using different ionic liquid-based lubricants, as described by Sharma et al. [18], the sulphur compounds of the tribofilm tend to be formed in the deeper layers. This explains why surface-sensitive techniques, such as XPS, do not detect sulphur, whereas techniques with deeper penetrations (e.g., EDS), do.

Regarding the XPS analysis of the worn surfaces after tribological tests with oil C, Table 8 shows that the most relevant feature found in the surface analysis of ATFs C, C0, and C1 was the relatively high content of bridging oxygen (P–O–P from polyphosphates) of sample C0 (15 %) compared to the other tested samples. The presence of these polyphosphates in C0 is probably related to its better performance in wear behaviour (Figure 8). Again, sulphur could not be detected on the surface, although this was expected considering that the concentration had to be even lower than that of the B series, where sulphur content was negligible.

Table 8. Peak positions, FWHM, and corresponding peaks assignments for O1s and P2p spectra under ATFs C, C0, and C1.

ATF	BE/eV	FWHM/eV	Area Percentage	Assigned to
		O1s		
C	531.6	2.1	52%	NBO
	532.8	2.2	9%	BO
	530.4	1.5	39%	Fe_3O_4
C0	531.9	2.1	55%	NBO
	532.7	2.0	15%	BO
	530.4	1.6	30%	Fe_3O_4
C1	531.7	2.3	64%	NBO
	533.4	2.5	2%	BO
	530.5	1.5	34%	Fe_3O_4
		P2p		
C	133.4	1.7	100%	$FePO_4$
C0	133.3	2.0	100%	$FePO_4$
C1	133.5	1.4	100%	$FePO_4$

4. Conclusions

The influences of additive concentrations on the electrical compatibilities and tribological behaviours of three commercial–automatic transmission fluids (ATFs A, B, and C) were studied. Measurements of electrical properties, such as electrical conductivity, permittivity, resistivity, dielectric dissipation factors at different temperatures, and dielectric breakdown voltage at room temperature were made. In addition, tribological properties were studied by both the so-called Stribeck curve and traction tests under rolling/sliding motions, as well as friction and wear tests under reciprocating motions. The main conclusions that can be drawn from the results are the following:

- Although the electric conductivity increased with the additive concentration, all the ATFs continued to have a dissipative character, and the breakdown voltage continued to be safe for application in EVs.
- The highest additive concentration used in ATFs B and C had a better antiwear performance than the original formulation without deteriorating the friction reduction and the electrical compatibility.
- The presence of iron phosphates and polyphosphates on the worn surface correlated with a better antiwear performance. Despite the presence of sulphur in the chemical compositions of some of the additive packages, the concentration of this element was too low to be detected by XPS on the worn surface.

Author Contributions: Conceptualization, A.H.B. and J.L.V.; methodology, A.H.B.; investigation, N.R., E.R., A.F.-G.; resources, E.R., A.H.B.; writing—original draft preparation, A.G.T., A.H.B., A.F.-G.; writing—review and editing, A.G.T., A.H.B., J.L.V.; visualization, A.G.T., E.R., A.F.-G.; supervision, A.H.B.; project administration, J.L.V.; funding acquisition, A.H.B. and J.L.V. All authors have read and agreed to the published version of the manuscript.

Funding: Ministry of Science, Innovation and Universities (Spain) and by the Government of the Principality of Asturias (Spain), grant numbers PID2019-109367RB-I00 and PA-21-AYUD/2021/50987, respectively.

Data Availability Statement: Not applicable.

Acknowledgments: The Scientific-Technical Services of the University of Oviedo is also acknowledged.

Conflicts of Interest: The authors declare no conflict of interest. The funders had no role in the design of the study; in the collection, analyses, or interpretation of data; in the writing of the manuscript; or in the decision to publish the results.

References

1. European Environment Agency. Trends and Projections in Europe. 2021. Available online: https://www.eea.europa.eu/publications/trends-and-projections-in-europe-2021 (accessed on 15 June 2022).
2. US EPA. Sources of Greenhouse Gas Emissions. Available online: https://www.epa.gov/ghgemissions/sources-greenhouse-gas-emissions#transportation (accessed on 15 June 2022).
3. Messerli, R.; Murniningtyas, E.; Eloundou-Enyegue, P.; Foli, E.G.; Furman, E.; Glassman, A.; Licona, G.H.; Kim, E.M.; Lutz, W.; Moatti, J.P. *Global Sustainable Development Report 2019: The Future Is Now—Science for Achieving Sustainable Development*; Department of Economic and Social Affairs of the United Nations (UNDESA): New York, NY, USA, 2019.
4. Woydt, M. The importance of tribology for reducing CO_2 emissions and for sustainability. *Wear* **2021**, *474–475*, 203768. [CrossRef]
5. COP26 Transport Declaration. Available online: https://cop26transportdeclaration.org/en/?contextKey=en#fulldeclaration (accessed on 15 June 2022).
6. Farfan-Cabrera, L.I. Tribology of electric vehicles: A review of critical components, current state and future improvement trends. *Tribol. Int.* **2019**, *138*, 473–486. [CrossRef]
7. Gangopadhyay, A.; Hanumalagutti, P.D. Challenges and Opportunities with Lubricants for HEV/EV Vehicles. In Proceedings of the STLE Annual Meeting, Nashville, TN, USA, 19–23 May 2019.
8. Gao, Z.; Salvi, L.; Flores-Torres, S. High Conductivity Lubricating Oils for Electric and Hybrid Vehicles. World Intellectual Property Organization (WIPO). International Bureau. Geneva, Switzerland. International Patent Number: WO 2018/067906 A1, 12 April 2018.
9. Flores-Torres, S.; Holt, D.G.L.; Carey, J.T. Method for Preventing or Minimizing Electrostatic Discharge and Dielectric Breakdown in Electric Vehicle Powertrains. World Intellectual Property Organization (WIPO). International Bureau. Geneva, Switzerland. International Patent Number: WO 2018/067905 A1, 12 April 2018.
10. Kwak, Y.; Cleveland, C.; Adhvaryu, A.; Fang, X.; Hurley, S.; Adachi, T. Understanding base oils and lubricants for electric drivetrain applications. *SAE Technol. Pap.* **2019**. [CrossRef]
11. Cao, H.; Meng, Y. Electrochemical effect on boundary lubrication of ZDDP additive blended in propylene carbonate/diethyl succinate. *Tribol. Int.* **2018**, *126*, 229–239. [CrossRef]
12. Yang, X.; Meng, Y.; Tian, Y. Effect of imidazolium ionic liquid additives on lubrication performance of propylene carbonate under different electrical potentials. *Tribol. Lett.* **2014**, *56*, 161–169. [CrossRef]
13. Yang, X.; Meng, Y.; Tian, Y. Potential-controlled boundary lubrication of stainless steels in non-aqueous sodium dodecyl sulfate solutions. *Tribol. Lett.* **2014**, *53*, 17–26. [CrossRef]
14. Rodríguez, E.; Rivera, N.; Fernández-González, A.; Pérez, T.; González, R.; Battez, A.H. Electrical compatibility of transmission fluids in electric vehicles. *Tribol. Int.* **2022**, *171*, 107544. [CrossRef]
15. Chen, Y.; Jha, S.; Raut, A.; Zhang, W.; Liang, H. Performance characteristics of lubricants in electric and hybrid vehicles: A review of current and future needs. *Front. Mech. Eng.* **2020**, *6*, 571464. [CrossRef]
16. Mcfadden, C.; Hughes, K.; Raser, L.; Newcomb, T. Electrical conductivity of new and used automatic transmission fluids. *Int. J. Fuels Lubr.* **2016**, *9*, 519–526. [CrossRef]
17. Sun, Y.B.; Zhang, Z.; Gong, Z.; Fan, Z.; Xu, Y. Temperature Dependence on Dielectric Properties of Automatic Transmission Fluid. In Proceedings of the 2022 IEEE 21st International Conference on Dielectric Liquids (ICDL), Sevilla, Spain, 29 May–2 June 2022. [CrossRef]
18. Sharma, V.; Gabler, C.; Doerr, N.; Aswath, P.B. Mechanism of tribofilm formation with P and S containing ionic liquids. *Tribol. Int.* **2015**, *92*, 353–364. [CrossRef]
19. Spikes, H. The history and mechanisms of ZDDP. *Tribol. Lett.* **2004**, *17*, 469–489. [CrossRef]
20. Grosseau-Poussard, J.L.; Panicaud, B.; Pedraza, F.; Renault, P.O.; Silvain, J.F. Iron oxidation under the influence of phosphate thin films. *J. Appl. Phys.* **2003**, *94*, 784–788. [CrossRef]
21. Mistry, K.K.; Morina, A.; Erdemir, A.; Neville, A. Tribological performance of EP lubricants with phosphorus-based additives. *Tribol. Trans.* **2013**, *56*, 645–651. [CrossRef]
22. Massoud, T.; De Matos, R.P.; Le Mogne, T.; Belin, M.; Cobian, M.; Thiébaut, B.; Loehlé, S.; Dahlem, F.; Minfray, C. Effect of ZDDP on lubrication mechanisms of linear fatty amines under boundary lubrication conditions. *Tribol. Int.* **2020**, *141*, 105954. [CrossRef]
23. Li, Y.; Li, Y.; Li, H.; Fan, X.; Yan, H.; Cai, M.; Xu, X.; Zhu, M. Insights into the tribological behavior of choline chloride–urea and choline chloride–thiourea deep eutectic solvents. *Friction* **2022**, 1–17. [CrossRef]